Geophys. J. Int. (1994) **119**, 949–963

The interpretation of shear-wave splitting parameters in the presence of two anisotropic layers

Paul G. Silver[1] and Martha K. Savage[2]

[1]*Department of Terrestrial Magnetism, Carnegie Institution of Washington, 5241 Broad Branch Road NW, Washington, DC 20015, USA*
[2]*Seismological Laboratory, MS 174, Mackay School of Mines, University of Nevada, Reno, NV 89557–0141, USA*

Accepted 1994 April 14. Received 1994 February 15; in original form 1993 February 2

SUMMARY

We consider the behaviour of shear-wave splitting parameters that are made under the assumption of a single layer of anisotropic material when in fact two layers of differing anisotropic properties are present. It is shown that the resulting *apparent* splitting parameters are still meaningful quantities and in fact can (at fixed frequency) be written as trigonometric functions of the splitting parameters of the individual layers. These expressions reveal many properties of the apparent splitting parameters. For example, the apparent fast polarization ϕ_a and delay time δt_a exhibit systematic variations as a function of incoming polarization with $\pi/2$ periodicity. The derived expressions can be used to invert for the individual properties of the two layers in many circumstances. We show that several stations along the San Andreas fault system display the properties of two layers, with the top layer being parallel to the local strike of the San Andreas fault. Finally, the derived expressions for the apparent splitting parameters are shown to be easily generalized to multiple layers.

Key words: anisotropy, San Andreas fault, shear-wave splitting.

INTRODUCTION

Since Hess (1964) discovered seismic anisotropy in the oceanic mantle, seismologists have been attempting to characterize the anisotropy of the crust and mantle. One of the least ambiguous methods of examining seismic anisotropy is through the method of shear-wave splitting, or birefringence. In this method, seismic anisotropy is characterized by the polarization ϕ of the leading shear wave, which yields the fast direction of anisotropy, and by the delay time δt between the fast and slow directions, which gives a measure of the product of the anisotropic path length and the degree of anisotropy (e.g. Nur & Simmons 1969; Crampin 1981). The last decade has seen an explosion in the number of shear-wave splitting observations, both from local and teleseismic events. Most such observations are made under a set of simplifying assumptions concerning the character of the anisotropic medium. In particular, it is usually assumed that the medium possesses hexagonal symmetry with a horizontal symmetry axis and that the anisotropy is localized in a single homogeneous layer beneath the receiver. Under these assumptions, ϕ and δt have the important properties of being only a weak function of incident angle and backazimuth for near vertical incidence (the case usually encountered for teleseismic *S* waves), and being independent of the polarization direction of the incoming shear wave for fixed incidence angle. Thus measurements from many events for a given station can be averaged together.

If a large enough range of arrival angles, backazimuths, and polarization directions is available, these assumptions can be tested. For example, a dipping symmetry axis will produce splitting parameters that possess 2π periodicity in backazimuth, as will the most general forms of laterally varying anisotropy. Even for a horizontal axis of symmetry, for large deviations from vertical, the splitting parameters will possess π periodicity (e.g. Crampin & Booth 1985). The existence of lower forms of symmetry, such as orthorhombic, rather than hexagonal, may produce large variations in splitting parameters even for rays coming in at near-vertical incidence. Finally, if two anisotropic layers are present, the splitting parameters become a function of polarization direction, even for fixed incidence angle.

It is this last violation of our simplifying assumptions that we focus on in the present report. We will show that the effects of two layers are sufficiently distinct from these other complications that they can be detected in many circumstances. Furthermore we will show that the apparent splitting parameters ϕ_a and δt_a obtained assuming one layer when in fact two are present, are still meaningful. In fact, ϕ_a

and δt_a can be written as explicit functions of the splitting parameters of the individual layers and the resulting expressions can be used to invert for these properties.

In the case of teleseismic shear waves, there are many situations where more than one anisotropic layer may be present along the path. The discovery of anisotropy beneath some subduction zone events (Kaneshima & Silver 1992; Russo & Silver) means that for certain records, there will be source- and receiver-side anisotropy. Secondly, if there is both 'fossil' anisotropy in the lithosphere (Silver & Chan 1988; Silver & Chan 1991; hereafter called SC) as well as anisotropy associated with asthenospheric flow, then there may be two anisotropic layers beneath the receiver. Finally, it may be that the crust and upper mantle have different anisotropic properties. The present report has in fact been motivated by a well-documented instance of inconsistent observations which, as we will argue, appear to indicate the existence of two layers.

METHOD

We assume that the action of an anisotropic layer is to split an incident shear-wave $\mathbf{u}(\omega)$ with polarization direction $\hat{\mathbf{p}}$ and propagation direction $\hat{\mathbf{b}}$ onto the fast and slow polarization directions $\hat{\mathbf{f}}$ and $\hat{\mathbf{s}}$ and then to time-shift these two components by $\delta t/2$ (earlier) and $-\delta t/2$ (later), respectively. For an elasticity tensor C_{ijkl}, $\hat{\mathbf{f}}$ and $\hat{\mathbf{s}}$ are the two quasi-shear eigenvectors of the polarization matrix $\mathbf{V}$ defined by

$$\rho V_{il} \equiv C_{ijkl}\hat{b}_j\hat{b}_k \tag{1}$$

(Backus 1965) with eigenvalues β_2^2 and β_1^2 corresponding to the two squared shear velocities. For small anisotropy, δt can be conveniently expressed in terms of a relative perturbation in shear velocity $\delta\hat{\beta} = \beta_0^{-1}(\delta\beta_1 - \delta\beta_2)$ as

$$\delta t = \beta_0^{-1} L \delta\hat{\beta}$$

where $\delta\beta_{1,2} = \beta_{1,2} - \beta_0$ and β_0 is the isotropic shear velocity defined such that $\delta\beta_1 + \delta\beta_2 = 0$.

Following SC, the effect of an anisotropic layer can be conveniently described by a splitting operator Γ, defined as:

$$\Gamma = e^{i\omega\delta t/2}\hat{\mathbf{f}}\hat{\mathbf{f}} + e^{-i\omega\delta t/2}\hat{\mathbf{s}}\hat{\mathbf{s}}. \tag{2}$$

Assuming a shear wave in an isotropic medium can be written as

$$\mathbf{u}(\omega) = w(\omega)\hat{\mathbf{p}}$$

where $w(\omega)$ is the wavelet function (Clarke & Silver 1991), then a split shear wave $\mathbf{u}_s(\omega)$ can be written

$$\mathbf{u}_s(\omega) = w(\omega)\Gamma \cdot \hat{\mathbf{p}}. \tag{3}$$

Following Yardley & Crampin (1991) we assume that the effect of two layers is to split the shear wave twice, into four individual phases (Fig. 1). This can be simply expressed by the application of 2 operators Γ_1 and Γ_2:

$$\mathbf{u}_s = w(\omega)\Gamma_2 \cdot \Gamma_1 \cdot \hat{\mathbf{p}} \tag{4}$$

where Γ_1 is the lower layer (applied first) and Γ_2 is the upper layer (applied second). Assuming that only one layer is present is equivalent to assuming that there exists an

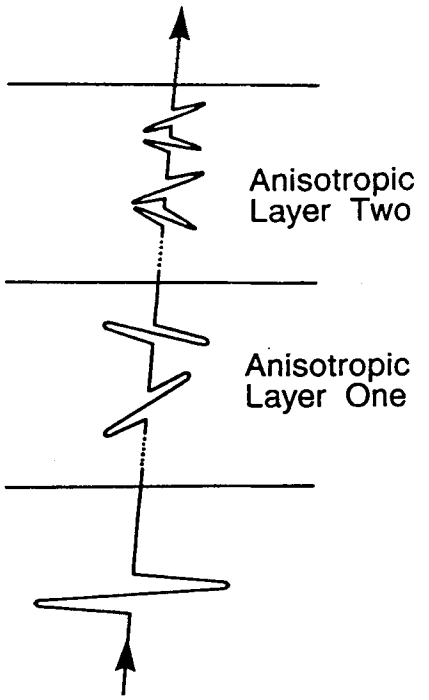

Figure 1. Schematic of shear-wave splitting in the case of two anisotropic layers. The incoming shear wave is split twice, leading to four individual waves at the receiver (from Yardley & Crampin 1991). In most cases the individual arrivals are unresolved.

apparent splitting operator Γ_a that satisfies the relation

$$\Gamma_2 \cdot \Gamma_1 \cdot \hat{\mathbf{p}} = K\Gamma_a \cdot \hat{\mathbf{p}} \tag{5}$$

where K is a (possibly frequency dependent) complex scalar to allow for an arbitrary time shift satisfying $|K| = 1$ (because the splitting operators are unitary), and where it is assumed that the initial polarization direction $\hat{\mathbf{p}}$ is known either from the phase type (e.g. *SKS, SKKS*), from a moment tensor for the event being studied, or from an estimate obtained directly from the data.

We seek to determine the properties of the apparent splitting parameters ϕ_a (the apparent direction of $\hat{\mathbf{f}}$) and δt_a measured under the assumption of a single anisotropic layer as a function of ϕ_p (the direction of $\hat{\mathbf{p}}$) and the splitting parameters of the two layers. If we let $\alpha_{1,2} = 2\phi_{1,2}$, where $\phi_{1,2}$ is the angle between ϕ_p and the fast polarization direction of layer (1, 2), let $\theta_{1,2} = \omega\delta t_{1,2}/2$, and define a_p, $a_{p_\perp}$, C_c, C_s by:

$$\begin{aligned} a_p &= \cos\theta_1\cos\theta_2 - \sin\theta_1\sin\theta_2\cos(\alpha_2 - \alpha_1) \\ a_{p_\perp} &= -\sin\theta_1\sin\theta_2\sin(\alpha_2 - \alpha_1) \\ C_c &= \cos\theta_1\sin\theta_2\cos\alpha_2 + \cos\theta_2\sin\theta_1\cos\alpha_1 \\ C_s &= \cos\theta_1\sin\theta_2\sin\alpha_2 + \cos\theta_2\sin\theta_1\sin\alpha_1 \end{aligned} \tag{6}$$

then, as shown in the Appendix, we can express the apparent splitting parameters α_a, θ_a as

$$\tan\alpha_a = \frac{a_{p_\perp}^2 + C_s^2}{a_{p_\perp}a_p + C_sC_c} \tag{7}$$

$$\tan\theta_a = \frac{a_{p_\perp}}{C_s\cos\alpha_a - C_c\sin\alpha_a} = \frac{C_s}{a_p\sin\alpha_a - a_{p_\perp}\cos\alpha_a}. \tag{8}$$

It is easily shown from (7)–(8) that the apparent splitting

parameters possess a $\pi/2$ periodicity in ϕ_p. This particular property is very important in distinguishing it from other sources of variation in two important ways (see introduction). First, if phases such as *SKS* are used (where ϕ_p is equal to backazimuth), the splitting parameters from these other mechanisms will not exhibit $\pi/2$ variation as a function of backazimuth. Secondly, for fixed-propagation direction, the splitting properties for these other mechanisms are independent of ϕ_p.

Extension to multiple layers

The above formulation can easily be extended to multiple layers. For N such layers (5) is replaced by

$$\left\{\prod_{n=1}^{N}\Gamma_n\right\}\cdot\hat{\mathbf{p}} = K\Gamma_a\cdot\hat{\mathbf{p}}.$$

As shown in the Appendix, the values of α_a and θ_a retain the form of (7) and (8), except that the coefficients are now given by

$$a_p = S\left[1 - \sum_{n=1}^{N-1}\sum_{n'=n+1}^{N}\tan\theta_n\tan\theta_{n'}\cos(\alpha_n-\alpha_{n'}) + \mathcal{O}(\tan^4\theta)\right]$$

$$a_{p_\perp} = S\left[\sum_{n=1}^{N-1}\sum_{n'=n+1}^{N}\tan\theta_n\tan\theta_{n'}\sin(\alpha_n-\alpha_{n'}) + \mathcal{O}(\tan^4\theta)\right]$$

$$C_c = S\left[\sum_{n=1}^{N}\tan\theta_n\cos\alpha_n + \mathcal{O}(\tan^3\theta)\right]$$

$$C_s = S\left[\sum_{n=1}^{N}\tan\theta_n\sin\alpha_n + \mathcal{O}(\tan^3\theta)\right]$$

where

$$S = \prod_{n=1}^{N}\cos\theta_n.$$

In the low-frequency limit only the terms proportional to $\tan\theta$ or $\tan^2\theta$ need to be retained.

PROPERTIES OF THE APPARENT SPLITTING PARAMETERS

These expressions provide some useful insights into the behaviour of the apparent splitting parameters. One important property is that for two layers, the splitting operators do not commute. While $a_p(1,2) = a_p(2,1)$, $C_c(1,2) = C_c(2,1)$, and $C_s(1,2) = C_s(2,1)$, we note that $a_{p_\perp}(1,2) = -a_{p_\perp}(2,1)$. Thus it is possible to determine which of two layers is on top as long as $a_{p_\perp}$ is non-zero. This is also illustrated in Fig. 2, which shows ϕ_a and δt_a as a function of polarization angle ϕ_p. The only difference between Figs 2(a), (b) and 2(c), (d) is that the order of the operators has been reversed.

Some other useful characteristics of $\phi_a(\phi_p)$ and $\delta t_a(\phi_p)$ are the following: (i) ϕ_a goes through a discontinuous jump of $-\pi/2$ when the denominator of (7) vanishes, as seen in Figs 2 and 3. Away from this jump, ϕ_a is a monotonically increasing function of ϕ_p, since its derivative

$$\mathrm{d}\phi_a/\mathrm{d}\phi_p = \frac{a_{p_\perp}^2}{(a_p a_{p_\perp} + C_s C_c)^2 + (a_{p_\perp}^2 + C_s^2)^2} \tag{9}$$

is always positive. (ii) $\delta t_a(\phi_p)$ reaches a maximum at a point near where the discontinuous jump in $\phi_a(\phi_p)$ occurs. (iii) There are 'null' directions (directions for which the particle motion is nearly linear and the particle motion direction remains unchanged) for particular values of the polarization direction ϕ_p. As shown in the Appendix, ϕ_p will approximately correspond to a null direction if $C_s = 0$ or

$$\frac{\tan\theta_2}{\tan\theta_1} = -\frac{\sin\alpha_1}{\sin\alpha_2}. \tag{10}$$

For example, if $\theta_1 = \theta_2$ (equal delay times in the two layers), the 'null' directions will be midway between the two fast polarization directions. As we will see in the next section, these regions are very important because they are near where abrupt changes in apparent splitting properties occur as a function of ϕ_p, the most revealing features of two anisotropic layers.

Other properties can be more easily seen in the low frequency limit $\theta_{1,2} \ll 1$. To first order in $\theta_{1,2}$, (7) and (8) become

$$\tan\alpha_a \sim \frac{C_s^2}{a_{p_\perp} + C_s C_c} \tag{11}$$

$$\tan\theta_a \sim \frac{C_s}{\sin\alpha_a} \tag{12}$$

[(12) is valid except when $\alpha_a \ll \theta_{1,2}$]. Perhaps surprisingly, the non-commutative nature of the two operators persists at low frequency because of the presence of $a_{p_\perp}$ which, like $C_s C_c$, is second order in θ. In this low-frequency limit, it is also useful to examine the special case of $\alpha_1 \sim \alpha_2$. To first order in $\delta\alpha = \alpha_2 - \alpha_1$,

$$\tan\alpha_a - \tan\alpha_1 \sim \delta\alpha\sec^2\alpha_1\hat{\theta}_2(2-\hat{\theta}_2) \tag{13}$$

where $\hat{\theta}_{1,2} = \theta_{1,2}/\theta$ and $\theta = \theta_1 + \theta_2$. Assuming $\sec^2\alpha_1$ is of order unity or less, this further simplifies to

$$\alpha_a \sim \alpha_1 + \delta\alpha\hat{\theta}_2(2-\hat{\theta}_2). \tag{14}$$

This illustrates that in this limit, α_a is a weighted average of α_1 and α_2. In the same limit, it is found that

$$\theta_a \sim \theta[1 + \delta\alpha\cot\alpha_1\hat{\theta}_2(\hat{\theta}_2 - 1)]. \tag{15}$$

Thus, θ_a is approximately the sum of the two delay times of the two layers. Equivalently, if $\phi_1 - \phi_2 \sim \pi/2$ then the delay times subtract. An example of this case is given in Fig. 3.

The strongest dependence of the apparent splitting parameters on ϕ_p occurs when $a_{p_\perp}$ is relatively large, i.e. $\delta t_1 \sim \delta t_2$ and $30° < \phi_2 - \phi_1 < 60°$. This is where we would expect to obtain the strongest constraints on the two layers. In contrast, weak dependence of the apparent splitting parameters on ϕ_p occurs for small $a_{p_\perp}$, which occurs when either $\delta t_{1,2} \gg \delta t_{2,1}$, (in which case $\phi_a \sim \phi_{1,2}$ and $\delta t_a \sim \delta t_{1,2}$), or ϕ_1 is approximately perpendicular or parallel to ϕ_2 (in which case the medium appears as one layer and the delay times add or subtract). Under these circumstances, it would be difficult to constrain the properties of the two layers. The relations (7) and (8) thus not only provide a way of predicting the behaviour of apparent splitting parameters, but also may be used as the basis for an inversion procedure to determine the splitting parameters of the individual layers, as shown below.

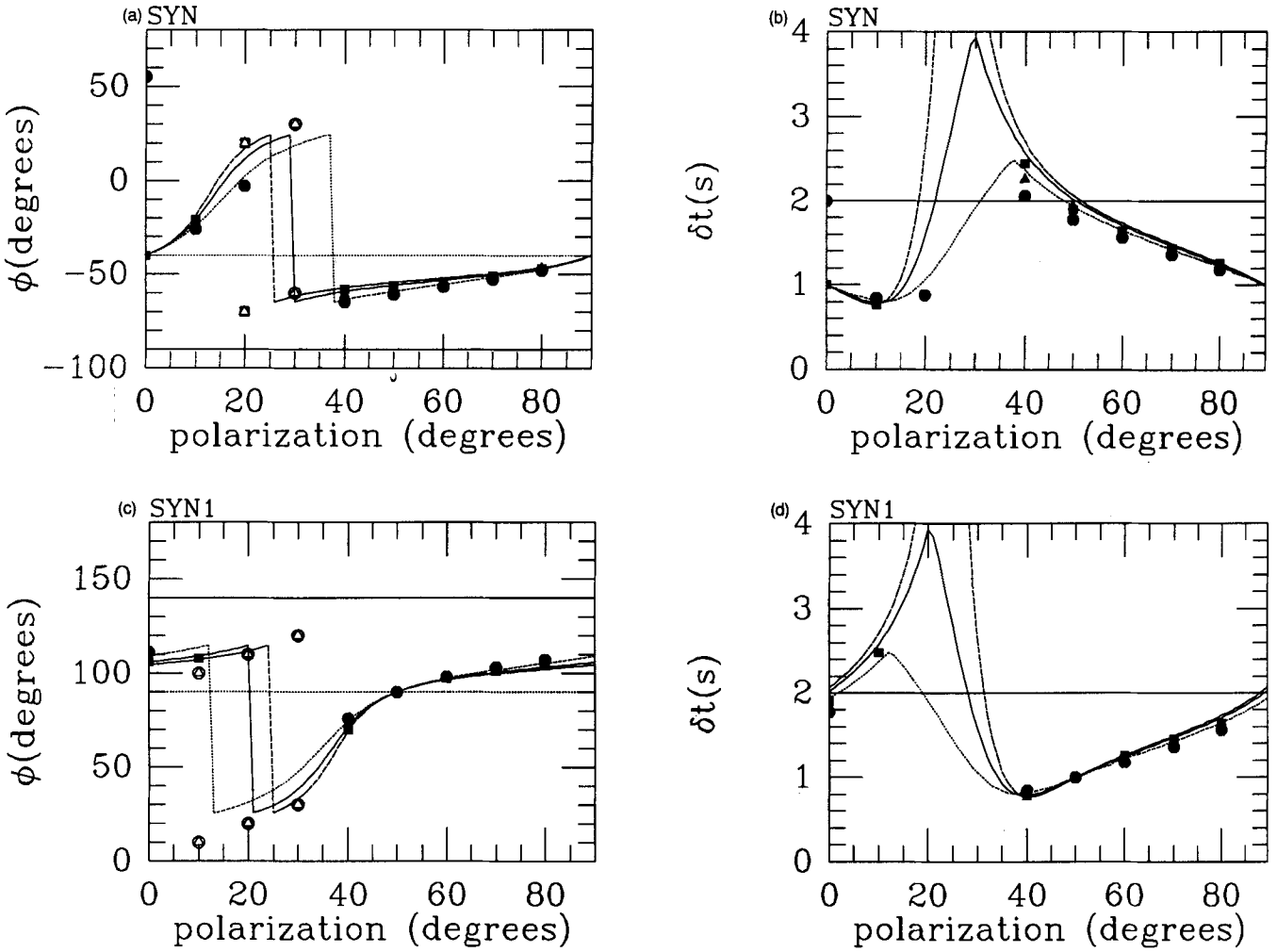

Figure 2. Curves for predicted apparent splitting parameters ϕ_a and δt_a as a function of incoming polarization direction ϕ_p using eqs (7)–(8). We consider two cases: (i) $\phi_1 = 90°(-90°)$ (bottom layer) and $\phi_2 = 140°(-40°)$ (top layer), $\delta t_1 = \delta t_2 = 1.0$ s for ϕ_a (a) and δt_a (b). (ii) Same as case (i) [ϕ_a (c) and δt_a (d)] except that ϕ_1 and ϕ_2 are reversed: $\phi_1 = 140°(-40°)$ (bottom layer) and $\phi_2 = 90°(-90°)$ (top layer). Straight lines are ϕ_1 (solid) and ϕ_2 (dotted). Curved lines are analytic results at periods of 5 s (dotted), 8 s (solid) and 20 s (dashed). Note that the two cases give very different results, illustrating that it is possible to determine which layer is on top even at low frequencies. Also shown, estimates of splitting parameters from synthetic data (using method of SC) generated using the splitting parameters for the two cases above (see also Figs 4 and 5). Filled symbols are well-constrained measurements, while open symbols are those that would normally be considered 'null' results. For nulls, ϕ is plotted as polarization direction ϕ_p and $\phi_p + 90°$. Measurements made on truncated sinusoids with period 5 s, 8 s, and 20 s denoted by circles, triangles and squares respectively. Note good correspondence between the measurements and analytic expressions.

Synthetic examples: two layers

In order to test the above expressions and to illustrate the effect of two anisotropic layers on seismic data, we have created synthetic wavelet functions consisting of one cycle of a sinusoid with a period of 8 s, the typical dominant period for the data we have been utilizing. We then estimated the apparent splitting parameters by the method of SC. Shown in Fig. 4 is such a doubly split shear wave with splitting parameters $\phi_1 = 90°(-90°)\delta t_1 = 1.0$ s, $\phi_2 = 140°(-40°)$, $\delta t_2 = 1.0$ s, and $\phi_p = 60°$ (angles measured clockwise from north). Note that, as predicted from the equations, for a frequency localized signal, one apparent operator is very successful in removing the anisotropy. The resulting value of ϕ_a is intermediate between the two values while δt_a is less than the sum of the delay times of the two layers. A second case is shown in Fig. 5 with the same splitting parameters but with $\phi_p = 30°$. This case is an example of a null result. Note that the particle motion is nearly linear, as expected. $\phi_p = 30°$ is close to the null value of $\phi_p = 25°$ predicted from (10).

Figure 2 compares measured apparent splitting parameters with the analytic expressions as a function of ϕ_p for two sets of splitting parameters. We note that the correspondence between the predicted values evaluated at 5 s, 8 s and 20 s period and the estimates from a truncated sinusoid with the same period is reasonably good, with the exception of the region where there is abrupt change in splitting properties. This is also the null region where splitting would not be detected. Finally, we have found that

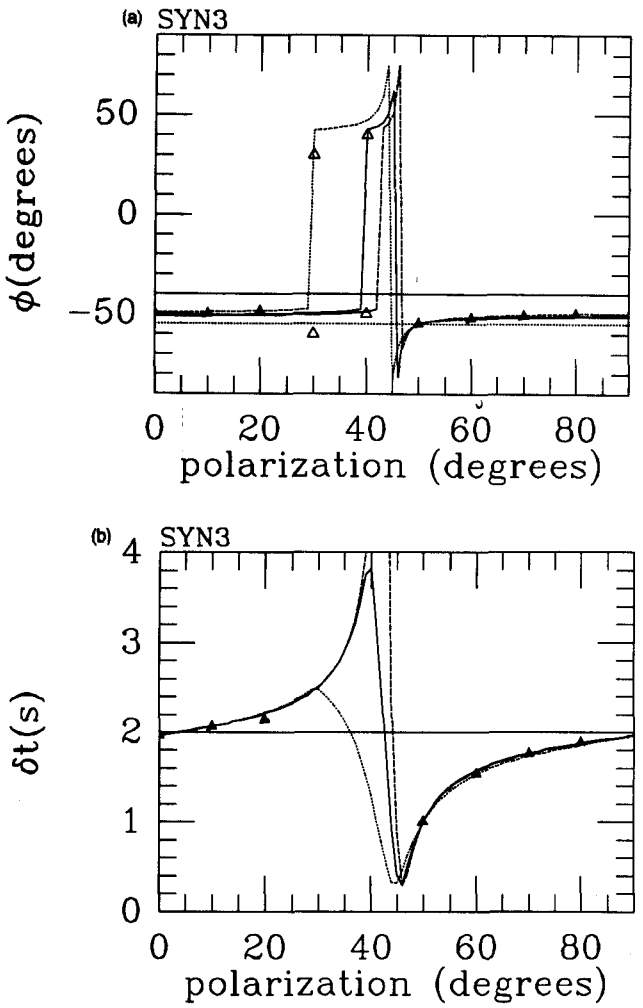

Figure 3. Same as Fig. 2(a), (b), except for a case when $\phi_1 \sim \phi_2$, i.e. $\phi_1 = -40°$ and $\phi_2 = -55°$, and $\delta t_1 = \delta t_2 = 1.0$ s.

using the measurement procedure of SC, that ϕ_p is typically estimated with errors of 10 per cent or less. Thus, for signals that are similarly localized in frequency, it is possible to use the analytic expressions to model the two layers.

Application to data

We have applied this technique to several stations along the San Andreas fault system: BKS, MHC and SAO (of the U.C. Berkeley Regional Network), which are within close proximity at the northern end of the fault, and which we group together as NSAN (Northern San ANdreas), and the station LAC (run by Lawrence Livermore National Labs; see Savage & Silver 1993 for details). We note from Fig. 6(a) that the splitting parameters, as a function of backazimuth, are well constrained (based on the error analysis of SC) but are internally inconsistent (see also Figs 2 and 3 of Savage & Silver 1993). As shown in Figs 6(b) and (c), however, as a function of polarization angle ϕ_p, the splitting parameters exhibit $\pi/2$ periodicity, which is most clearly shown by the simplicity of Fig. 6(c) in which ϕ_a and δt_a are plotted versus ϕ_p modulo $\pi/2$. We have used the expressions for apparent splitting parameters given in the previous section to retrieve the splitting parameters from each layer by searching for those values that best fit the measured values of ϕ and δt as a function of ϕ_p. For the calculated values, we used a period of 8 s, corresponding to the dominant period of most of the records at NSAN and LAC (see Figs 2 and 3 of Savage & Silver 1993). The criteria weighted most heavily in our qualitative fits to the data were the location of the 'jumps' and the trends of the plots.

The best-fitting parameters are $(\phi_1, \delta t_1) = (90°, 0.9\text{ s})$, $(\phi_2, \delta t_2) = (140°, 1.1\text{ s})$ for NSAN and $(\phi_1, \delta t_1) = (60°, 0.6\text{ s})$, $(\phi_2, \delta t_2) = (110°, 0.8\text{ s})$ for LAC. There is some trade-off between the parameters that limits the accuracy of these measurements to about $\pm 25°$ in ϕ_a and ± 0.3 s in δt_a (see Savage & Silver 1993 for discussion). The major features of the data, the $\pi/2$ periodicity and the position and direction of the jumps in δt_a and ϕ_a are fit well at both stations. That such a simple four-parameter model does such a good job of accounting for the data suggests that we are modelling the correct phenomenon. The most noticeable misfit is between the measured and calculated ϕ_a at NSAN over the range from 35 to 70 degrees in ϕ_p, where the data are systematically lower than the predicted values. This may indicate that our model is too simplistic. Possible modifications could include a dipping symmetry axis, or laterally varying anisotropy, in one of the layers (see also Ozalaybey & Savage 1994, for a direct, waveform inversion of the data).

The results are tectonically intriguing, in that for both NSAN and LAC the upper layer is locally parallel to the strike of the San Andreas fault, although the lower layer is at a high angle to this direction (see Savage & Silver 1993, for tectonic discussion). Thus far, no other stations we have examined appear to require the presence of two layers.

CONCLUSION

The expressions we have developed for the properties of observed splitting parameters measured under the assumption of one layer, when in fact two layers are present, allow for the interpretation of splitting parameters in more complex media. The actual measurements still have meaning in that they can be related in a straightforward manner to the splitting parameters of the two layers. We have shown that the dependence of the apparent splitting parameters on incoming polarization can be used to invert for the splitting properties of the two layers. Such models can in principle be tested under certain circumstances. If the two layers are in contact, then the properties of the converted phases at the interface between two anisotropic layers can be predicted (Farra *et al.* 1991). Finally, the fact that for most kinds of data, the individual observations are well behaved for the two-layer case, emphasizes the importance of obtaining, if possible, precise splitting parameters for a wide range of polarization directions and looking carefully for the diagnostics of two layers.

ACKNOWLEDGMENTS

We thank S. Ozalaybey, S. Crampin, J. P. Montagner and V. Farra for useful discussions during the writing of this manuscript. We also thank P. Shearer for a helpful review. G. Zandt and C. Short of Lawrence Livermore National Laboratories, and R. Uhrhammer and R. McKenzie of University of California, Berkeley, for providing much of the data for this study. The work has been supported by the

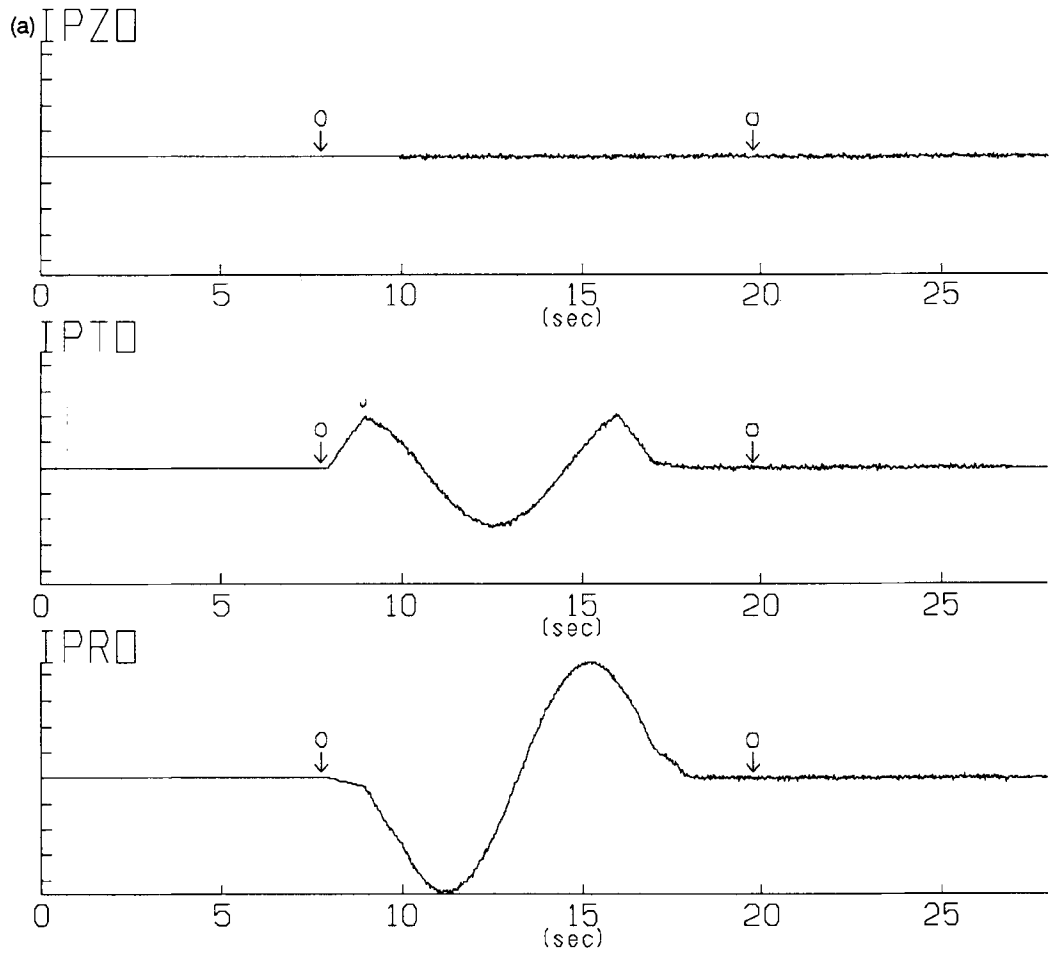

Figure 4. Illustration of the effect of two layers on seismic data. (a) Synthetic data consists of a truncated sinusoid (8 s period) plus Gaussian random noise on the radial component, which has been split twice with splitting parameters $\phi_1 = 90°$ $\delta t_1 = 1.0$ s, $\phi_2 = 140°$, $\delta t_2 = 1.0$ s, backazimuth = 60°. For a vertically propagating wave, the resulting waveforms are shown for the vertical (top, no signal), transverse (middle) and radial (bottom) components. Circles with arrows mark the interval used to make the measurement. The estimated apparent splitting parameters are found to be $\phi_a = -55°$ (125°) and $\delta t_a = 1.6$ s. (b) Two top traces: original transverse and radial components. Bottom two traces: corrected components. (c) Top two traces: superposition of fast (ϕ_a) and slow components ($\phi_a + 90°$) uncorrected (left) and corrected (right). Bottom: particle motion for fast and slow components uncorrected (left) and corrected (right). Corrections made using estimated values of (ϕ_a, δt_a). (d) Contour plot of the energy on the corrected transverse component as a function of ϕ_a and δt_a. Minimum value (dot) shown with 95 per cent confidence region (double contour) and multiples of that contour level. Note that a single splitting operator does a very good job of accounting for the splitting, with the possible exception of unmodelled high-frequency energy at the ends of the waveform (b and c).

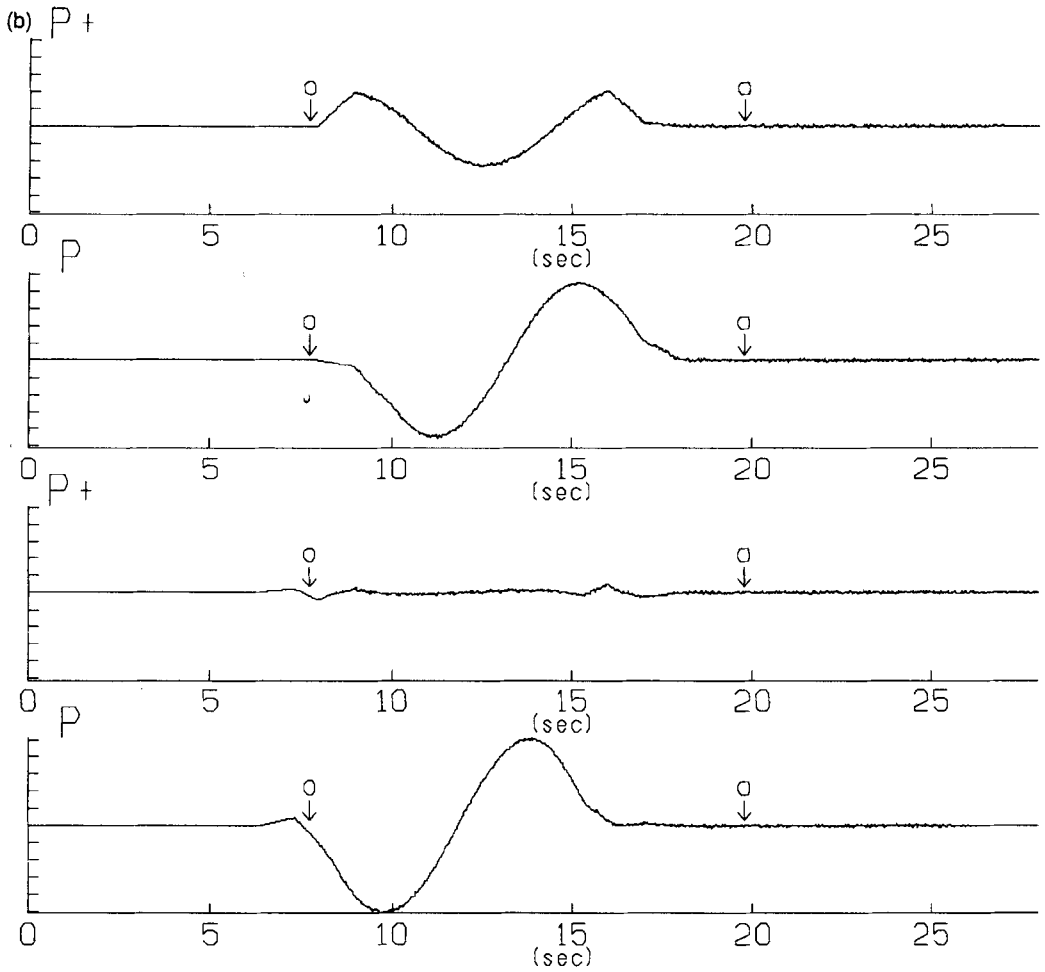

Figure 4. (*Continued.*)

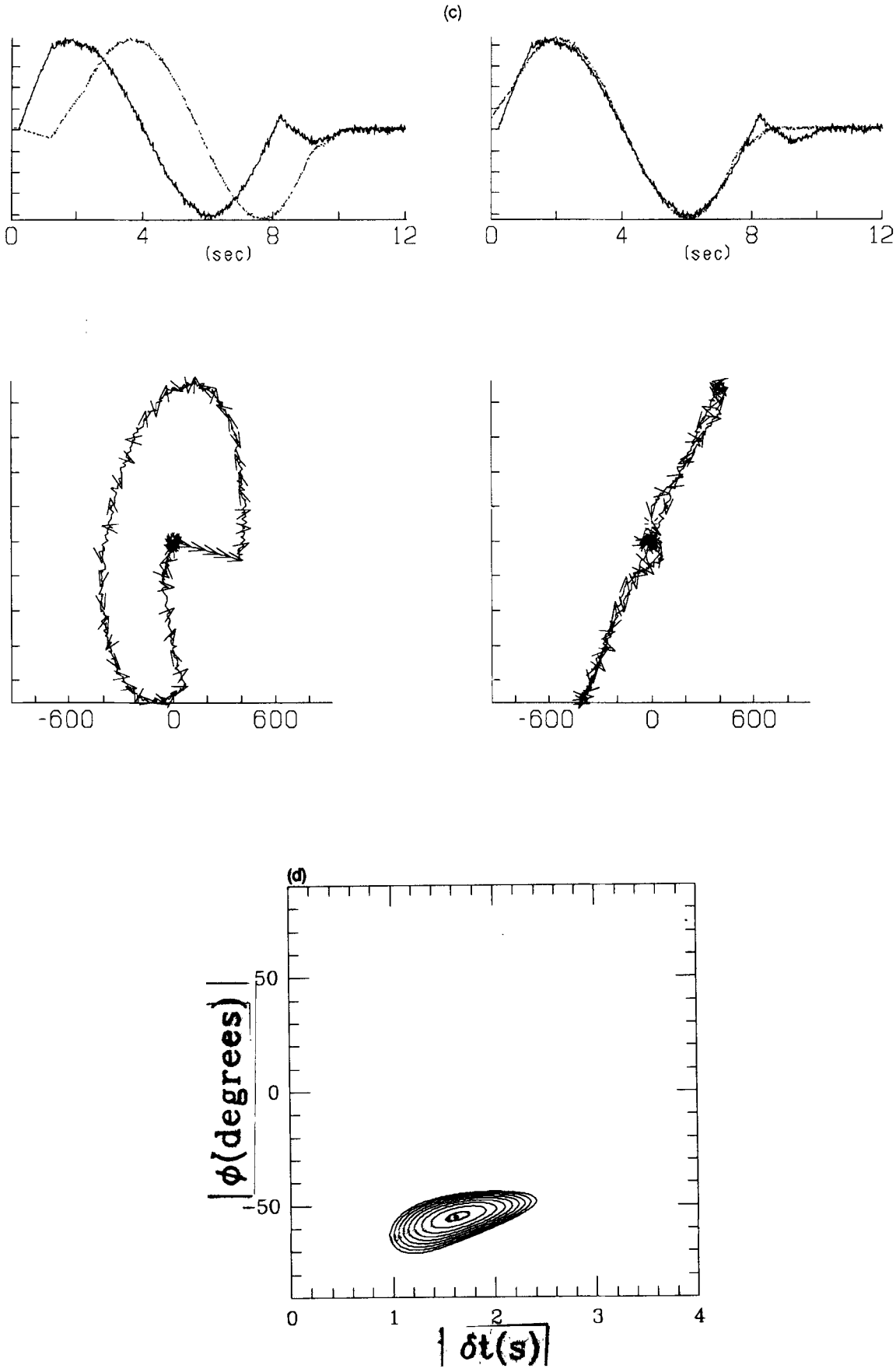

Figure 4. (*Continued.*)

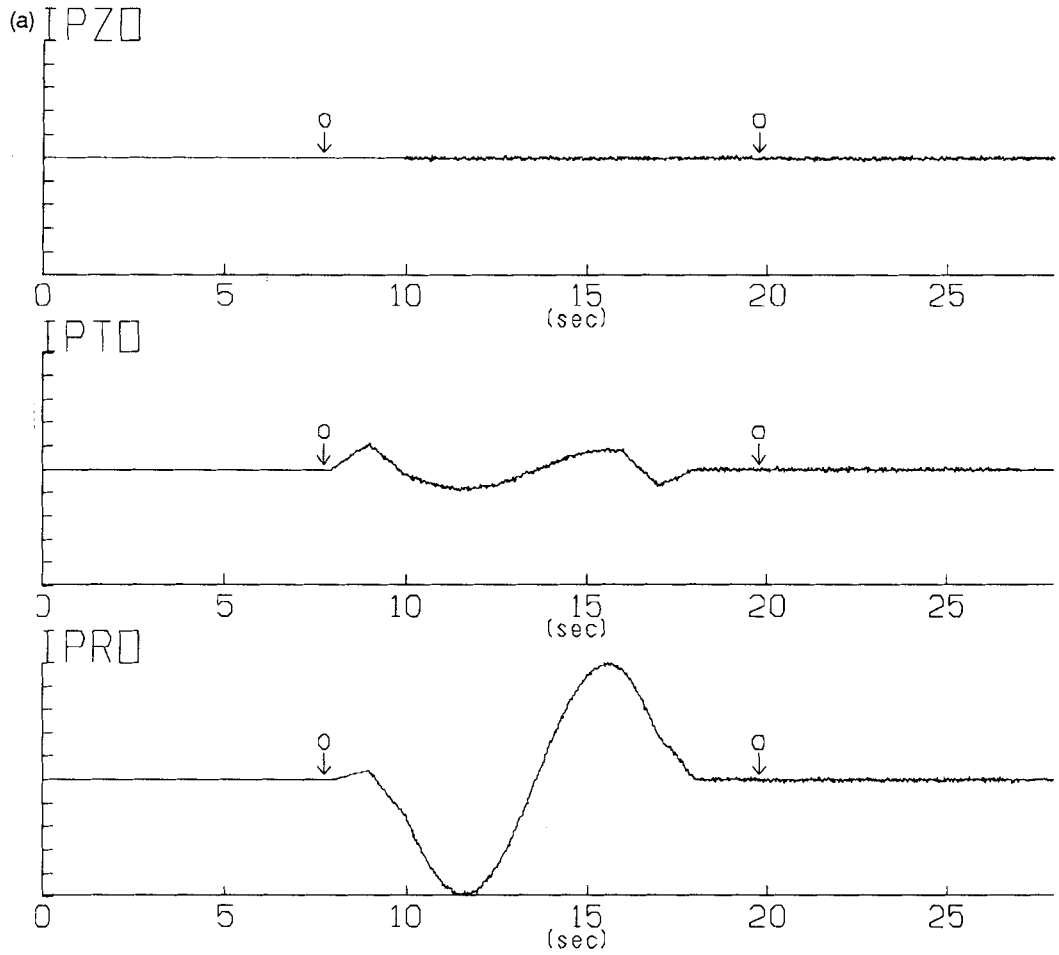

Figure 5. Same as Fig. 4 except that the backazimuth is 30°. In this case, however, no splitting is detected (which we refer to as a 'null' result). This is close to the predicted null direction of 25° given by eq. (10) (see text for details).

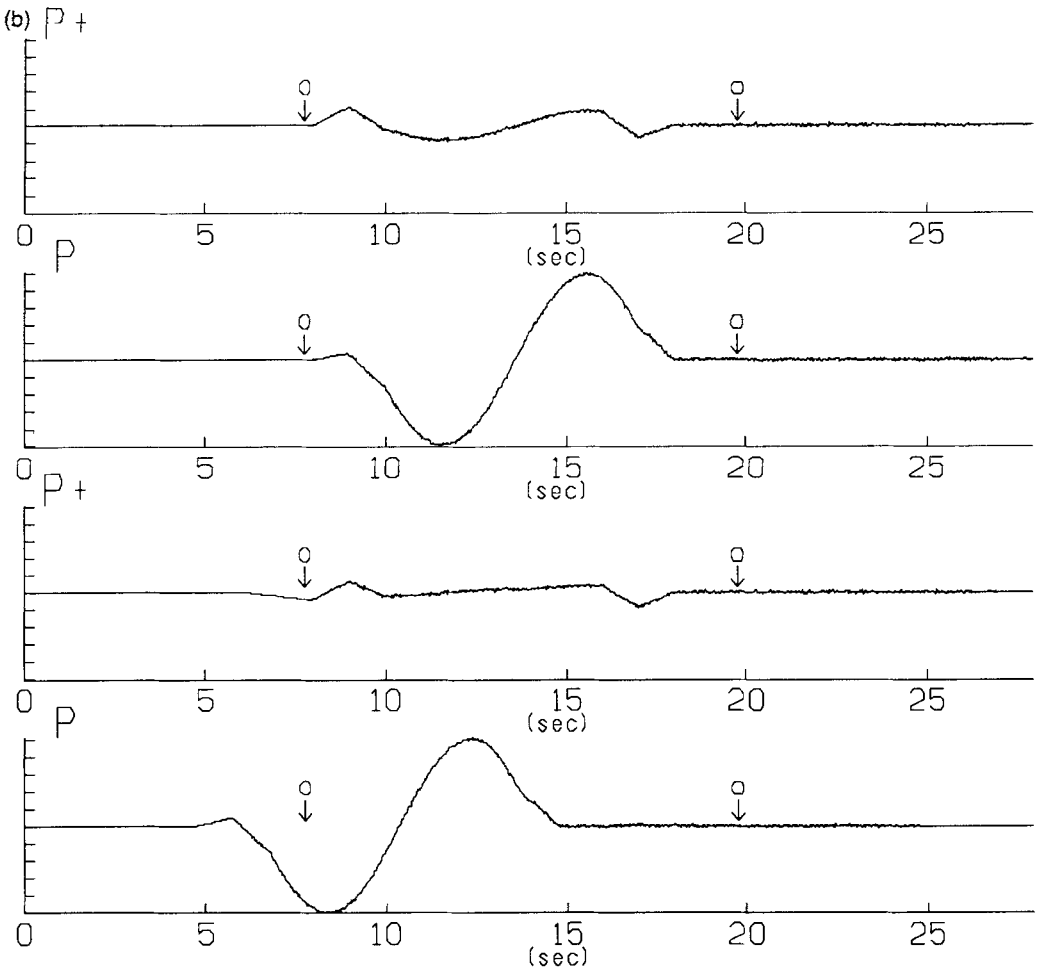

Figure 5. (*Continued.*)

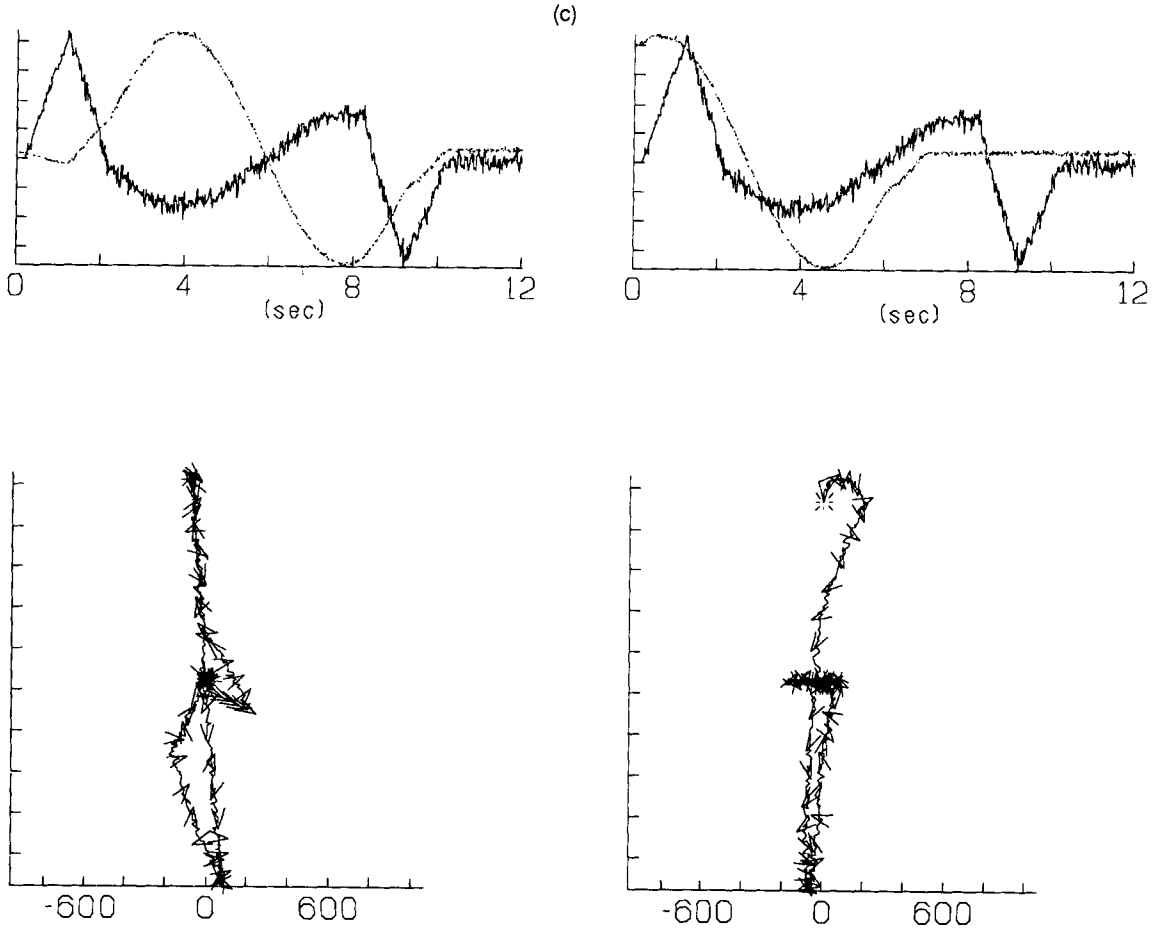

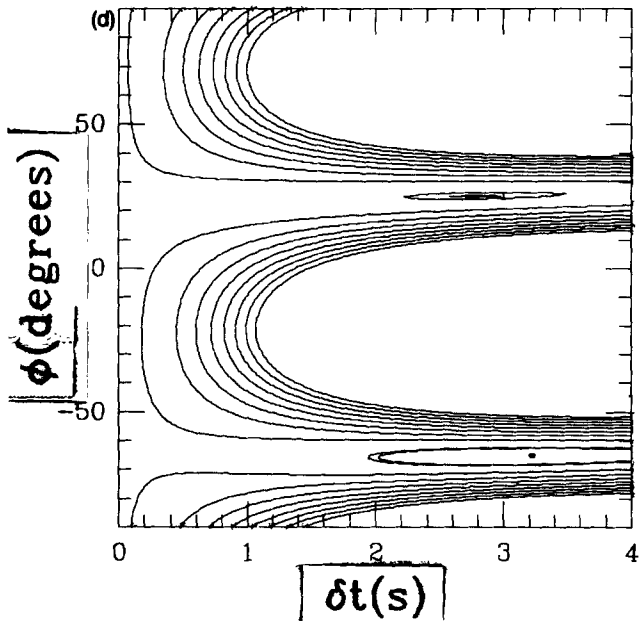

Figure 5. (*Continued.*)

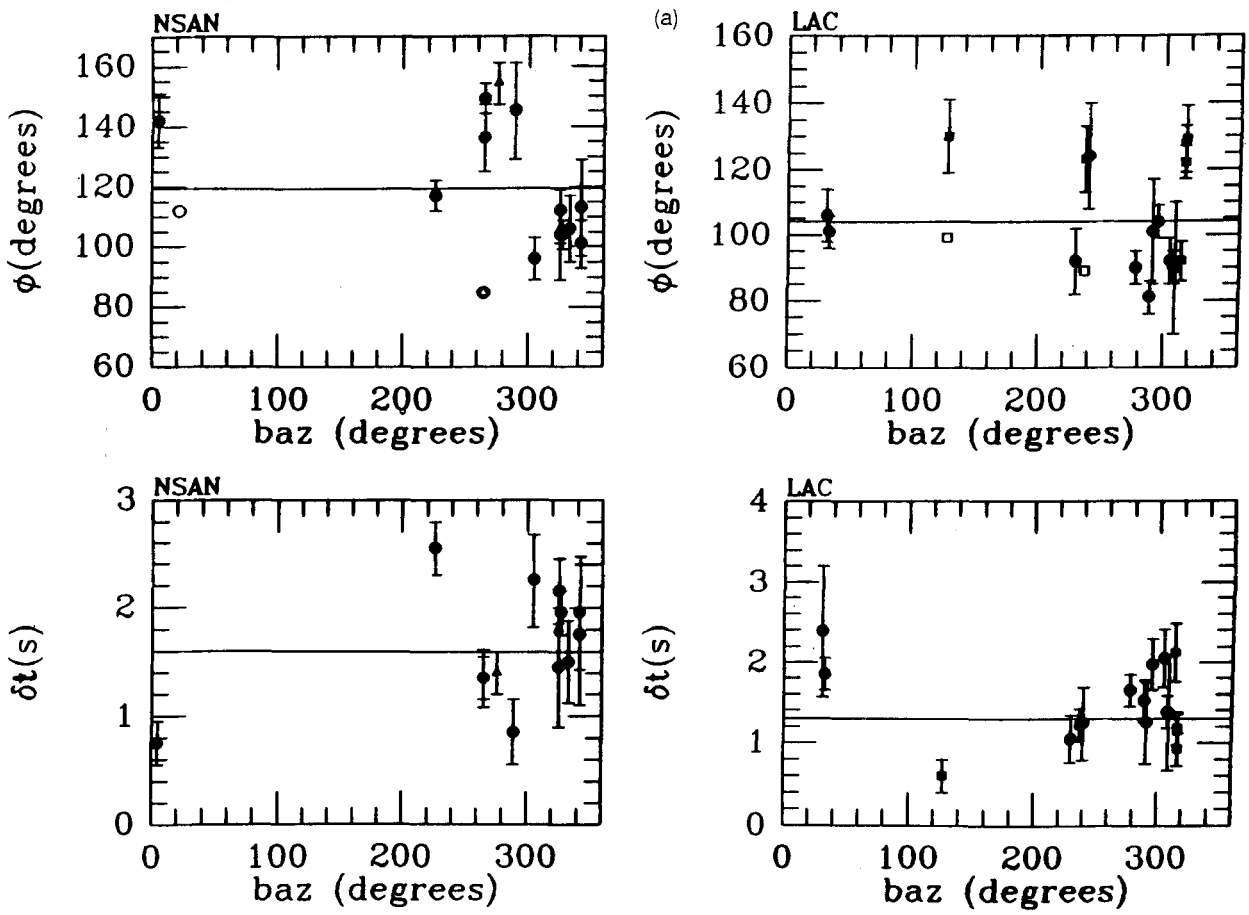

Figure 6. High-quality measurements of ϕ and δt as a function of backazimuth from stations MHC, BKS, and SAO along the northern San Andreas fault (NSAN), and station LAC. Circles are *SKS*, triangles *SKKS*, and squares *S*. Closed symbols represent well-constrained observations of splitting, while open symbols represent cases where splitting is not detectable (null measurements). In this second case, ϕ is plotted as polarization direction ϕ_p and $\phi_p + 90°$. Solid horizontal line gives weighted average values of ϕ and δt. (b) High-quality individual measurements of ϕ and δt as a function of polarization direction ϕ_p modulo 180° from NSAN and LAC. Compare with (a) and note the clear systematic pattern that has emerged, with a period of 90°. Also included are curves calculated for the double-layer anisotropic parameters given in text. Symbols are the same as in (a). (c) Same as (b) but modulo 90°. Note that this simple four-parameter model fits the observations reasonably well.

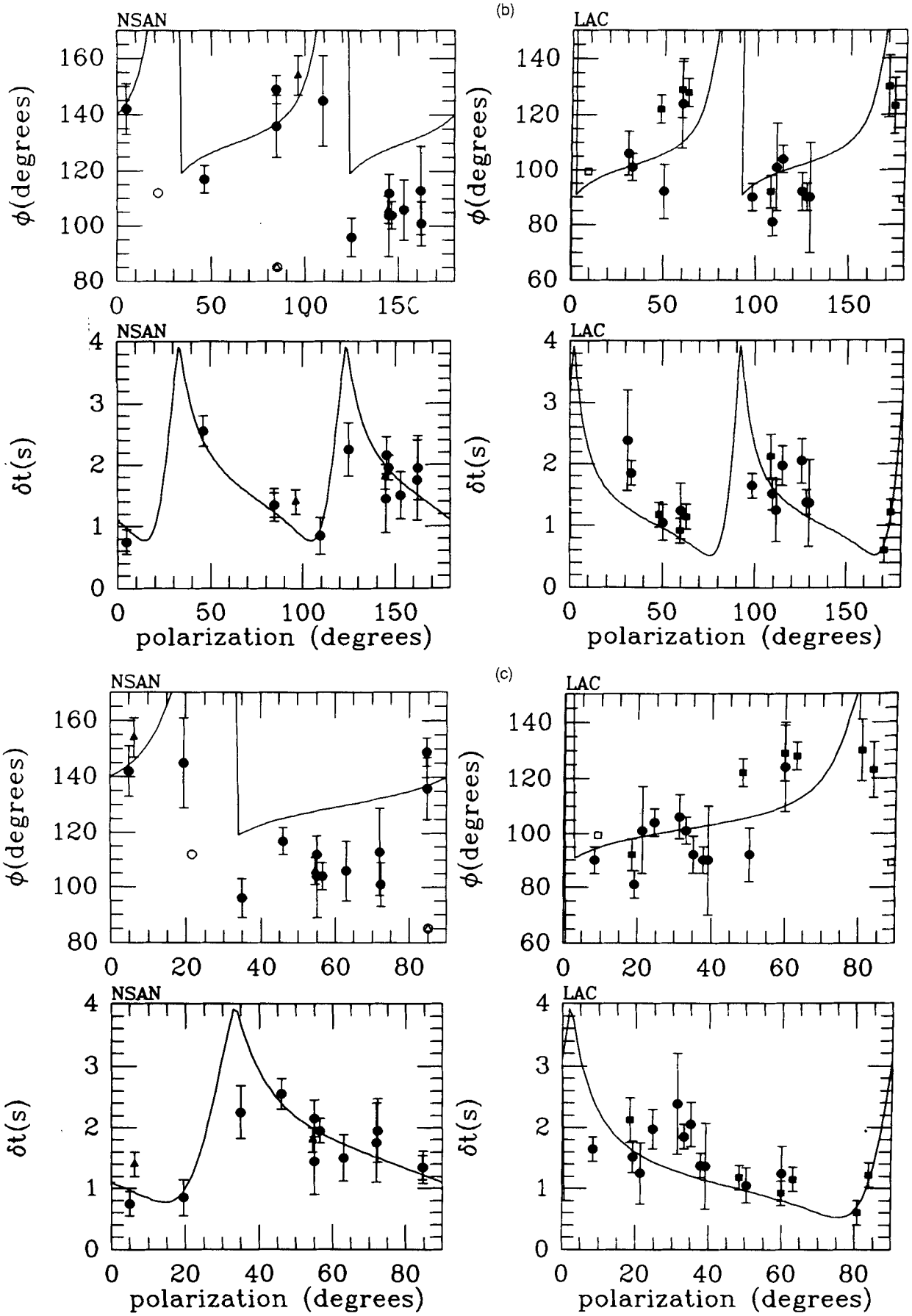

Figure 6. (*Continued.*)

United States National Science Foundation grant EAR-8917161, US Geological Survey grants 14-08-0001-G1973 and 14-08-0001-A0618, and the Carnegie Institution of Washington, DTM.

REFERENCES

Backus, G.E., 1965. Possible forms of seismic anisotropy of the uppermost mantle under oceans, *J. geophys. Res.*, **70,** 3429–3439.

Clarke, T.J. & Silver, P.G., 1991. A procedure for the systematic interpretation of body wave seismograms, 1. Application to Moho depth and crustal properties, *Geophys. J. Int.*, **104,** 41–72.

Crampin, S., 1981. A review of wave motion in anisotropic and cracked elastic-media, *Wave Motion,* **3,** 343–391.

Crampin, S. & Booth, D.C., 1985. Shear-wave polarizations near the North Anatolian Fault—II. Interpretation in terms of crack-induced anisotropy, *Geophys. J. R. astr. Soc.,* **83,** 75–92.

Farra, V., Vinnik, L.P., Romanowicz, B., Kosarev, G.L. & Kind, R., 1991. Inversion of teleseismic *S* particle motion for azimuthal anisotropy in the upper mantle: a feasibility study, *Geophys. J. R. astr. Soc.,* **106,** 421–431.

Hess, H.H., 1964. Seismic anisotropy of the uppermost mantle under oceans, *Nature,* **203,** 629–631.

Kaneshima, S. & Silver, P.G., 1992. A search for source-side anisotropy, *Geophys. Res. Lett.,* **19,** 1049–1052.

Nur, A. & Simmons, G., 1969. Stress-induced velocity anisotropy in rock: an experimental study, *J. geophys. Res.,* **74,** 6667–6674.

Ozalaybey, S. & Savage, M.K., 1994. Double layer anisotropy resolved from *S* phases, *Geophys. J. Int.,* **117,** 653–664.

Savage, M. & Silver, P.G., 1993. Mantle deformation and tectonics: constraints from seismic anisotropy in western United States, *Phys. Earth planet Inter.,* **78,** 207–227.

Silver, P.G. & Chan, W.W., 1988. Implications for continental structure and evolution from seismic anisotropy, *Nature,* **335,** 34–39.

Silver, P.G. & Chan, W.W., 1991. Shear-wave splitting and subcontinental mantle deformation, *J. geophys. Res.,* **96,** 16 429–16 454.

Yardley, G.S. & Crampin, S., 1991. Extensive-dilatancy anisotropy: relative information in VSPs and reflection surveys, *Geophys. Prospect.,* **39,** 337–355.

APPENDIX

Expressions for apparent splitting parameters

Two-layer case

It is convenient to write the splitting operator Γ, defined in (2), as

$$\Gamma = \cos\theta\mathbf{I} + i\sin\theta\boldsymbol{\sigma} \tag{A1}$$

where $\theta = \omega\delta t/2$, $\mathbf{I}$ is the identity and $\boldsymbol{\sigma} = \hat{\mathbf{f}}\hat{\mathbf{f}} - \hat{\mathbf{s}}\hat{\mathbf{s}}$. If we consider the coordinate system defined by the initial polarization direction $\hat{\mathbf{p}}$ and the perpendicular direction $\hat{\mathbf{p}}_\perp$, then we can express σ as

$$\boldsymbol{\sigma} = \cos\alpha\mathbf{e}_a + \sin\alpha\mathbf{e}_b \tag{A2}$$

where $\alpha = 2\phi$ and ϕ is the angle between the fast polarization direction $\hat{\mathbf{f}}$ and the initial polarization direction $\hat{\mathbf{p}}$ and

$$\begin{aligned}\mathbf{e}_a &\equiv \hat{\mathbf{p}}\hat{\mathbf{p}} - \hat{\mathbf{p}}_\perp\hat{\mathbf{p}}_\perp\\ \mathbf{e}_b &\equiv \hat{\mathbf{p}}\hat{\mathbf{p}}_\perp + \hat{\mathbf{p}}_\perp\hat{\mathbf{p}}.\end{aligned} \tag{A3}$$

Then Γ can be written as

$$\Gamma = \cos\theta\mathbf{I} + i\sin\theta[\cos\alpha\mathbf{e}_a + \sin\alpha\mathbf{e}_b]. \tag{A4}$$

Thus, the dot product of the two operators can be written

$$\Gamma_2\cdot\Gamma_1 = [\cos\theta_2\mathbf{I} + i\sin\theta_2(\cos\alpha_2\mathbf{e}_a + \sin\alpha_2\mathbf{e}_b)]\cdot$$
$$[\cos\theta_1\mathbf{I} + i\sin\theta_1(\cos\alpha_1\mathbf{e}_a + \sin\alpha_1\mathbf{e}_b)]$$

which, using relations (A3) can be written as

$$\begin{aligned}\Gamma_2\cdot\Gamma_1 = {}&[\cos\theta_1\cos\theta_2 - \sin\theta_1\sin\theta_2\cos(\alpha_2-\alpha_1)]\mathbf{I}\\ &+ i[(\cos\theta_1\sin\theta_2\cos\alpha_2 + \cos\theta_2\sin\theta_1\cos\alpha_1)\mathbf{e}_a\\ &+ (\cos\theta_1\sin\theta_2\sin\alpha_2 + \cos\theta_2\sin\theta_1\sin\alpha_1)\mathbf{e}_b]\\ &+ \sin\theta_1\sin\theta_2\sin(\alpha_2-\alpha_1)\mathbf{e}_c\end{aligned} \tag{A5}$$

where $\mathbf{e}_c \equiv \mathbf{e}_a\cdot\mathbf{e}_b = -\mathbf{e}_b\cdot\mathbf{e}_a = \hat{\mathbf{p}}\hat{\mathbf{p}}_\perp - \hat{\mathbf{p}}_\perp\hat{\mathbf{p}}$. Using (A5) and noting that $\mathbf{e}_a\cdot\mathbf{e}_a = \mathbf{e}_b\cdot\mathbf{e}_b = \mathbf{I}$,

$$\Gamma_2\cdot\Gamma_1\cdot\hat{\mathbf{p}} = (a_p + iC_c)\hat{\mathbf{p}} + (a_{p_\perp} + iC_s)\hat{\mathbf{p}}_\perp \tag{A6}$$

where

$$\begin{aligned}a_p &= \cos\theta_1\cos\theta_2 - \sin\theta_1\sin\theta_2\cos(\alpha_2-\alpha_1)\\ a_{p_\perp} &= -\sin\theta_1\sin\theta_2\sin(\alpha_2-\alpha_1)\\ C_c &= \cos\theta_1\sin\theta_2\cos\alpha_2 + \cos\theta_2\sin\theta_1\cos\alpha_1\\ C_s &= \cos\theta_1\sin\theta_2\sin\alpha_2 + \cos\theta_2\sin\theta_1\sin\alpha_1\end{aligned}$$

(same as eq. 6 in body of text). We seek an operator such that

$$\Gamma_2\cdot\Gamma_1\cdot\hat{\mathbf{p}} = \Gamma_a\cdot\mathbf{p}' \tag{A7}$$

where $\mathbf{p}'$ is defined as

$$\mathbf{p}' = K[\cos\gamma\hat{\mathbf{p}} + \sin\gamma\hat{\mathbf{p}}_\perp] \tag{A8}$$

K is a complex scalar (which allows for an arbitrary time shift) of unit norm (because the splitting operators are unitary), and the angle γ allows for a possible apparent rotation of the initial polarization vector. In this case, using eq. (A4),

$$\begin{aligned}\Gamma_a\cdot\mathbf{p}' &= K\{\cos\theta_a[\cos\gamma\hat{\mathbf{p}} + \sin\gamma\hat{\mathbf{p}}_\perp]\\ &\quad + i\sin\theta_a[\cos\alpha_a(\cos\gamma\hat{\mathbf{p}} - \sin\gamma\hat{\mathbf{p}}_\perp)\\ &\quad + \sin\alpha_a(\cos\gamma\hat{\mathbf{p}}_\perp + \sin\gamma\hat{\mathbf{p}})]\}\\ &= K[\{\cos\theta_a\cos\gamma + i\sin\theta_a[\cos\alpha_a\cos\gamma\\ &\quad + \sin\alpha_a\sin\gamma]\}\hat{\mathbf{p}}\\ &\quad + \{\cos\theta_a\sin\gamma + i\sin\theta_a[-\cos\alpha_a\sin\gamma\\ &\quad + \sin\alpha_a\cos\gamma]\}\hat{\mathbf{p}}_\perp].\end{aligned} \tag{A9}$$

Equating the terms proportional to $\hat{\mathbf{p}}$ and $\hat{\mathbf{p}}_\perp$:

$$\begin{aligned}K[\cos\theta_a\cos\gamma + i\sin\theta_a\cos(\alpha_a-\gamma)] &= a_p + iC_c\\ K[\cos\theta_a\sin\gamma + i\sin\theta_a\sin(\alpha_a-\gamma)] &= a_{p_\perp} + iC_s.\end{aligned} \tag{A10}$$

Note that there are four unknowns: θ_a, α_a, γ and the phase of K. Although there appear to be four equations (real and imaginary parts of the coefficients multiplying $\hat{\mathbf{p}}$, $\hat{\mathbf{p}}_\perp$), only three of these are independent, since $a_p^2 + a_{p_\perp}^2 + C_c^2 + C_s^2 = 1$. In most cases we can fix $\gamma = 0$. For example, the initial polarization can be known either because of phase type (such as with *SKS*) or from a moment tensor. More generally, it can be shown that γ is a quadratic function of frequency, so that in the low-frequency limit it will be very small. This means that $\hat{\mathbf{p}}$ can be estimated directly from the

data with little error, so that γ will be typically close to zero. Using this value of γ in (A10) and eliminating K leads to

$$\frac{a_p + iC_c}{\cos\theta_a + i\sin\theta_a\cos\alpha_a} = \frac{a_{p_\perp} + iC_s}{i\sin\theta_a\sin\alpha_a}.$$

Multiplying by $\cos\theta_a$ and equating real and imaginary parts,

$$-\sin\alpha_a C_c\tan\theta_a = a_{p_\perp} - \cos\alpha_a C_s\tan\theta_\alpha \quad \text{(A11a)}$$

$$\sin\alpha_a a_p\tan\theta_a = C_s + \cos\alpha_a a_{p_\perp}\tan\theta_a \quad \text{(A11b)}$$

which yields

$$\tan\theta_a = \frac{a_{p_\perp}}{C_s\cos\alpha_a - C_c\sin\alpha_a} \quad \text{(A12a)}$$

or

$$\tan\theta_a = \frac{C_s}{a_p\sin\alpha_a - a_{p_\perp}\cos\alpha_a}. \quad \text{(A12b)}$$

Using (A12) to eliminate θ_a and solving for α_a,

$$\tan\alpha_a = \frac{a_{p_\perp}^2 + C_s^2}{a_{p_\perp}a_p + C_sC_c}. \quad \text{(A13)}$$

Once α_a is found, (A12) can be used to compute θ_a.

Generalization to multiple layers. In the case of multiple layers, the above formalism can be easily generalized. In place of (5) we substitute

$$\left\{\prod_{n=1}^{N}\Gamma_n\right\}\cdot\hat{\mathbf{p}} = K\Gamma_a\cdot\hat{\mathbf{p}} \quad \text{(A14)}$$

for N layers. Using (A1) in (A14) and defining

$$S = \prod_{n=1}^{N}\cos\theta_n$$

$$\left\{\prod_{n=1}^{N}\Gamma_n\right\}\cdot\hat{\mathbf{p}} = S\Bigg[\mathbf{I} + i\sum_{n=1}^{N}\tan\theta_n\sigma_n - \sum_{n=1}^{N-1}\sum_{n'=n+1}^{N}\tan\theta_n\tan\theta_{n'}\sigma_n\cdot\sigma_{n'} - i\sum_{n=1}^{N-2}\sum_{n'=n+1}^{N-1}\sum_{n''=n'+1}^{N}\tan\theta_n\tan\theta_{n'} \times\tan\theta_{n''}\sigma_n\cdot\sigma_{n'}\cdot\sigma_{n''} + \cdots\Bigg]\cdot\hat{\mathbf{p}}. \quad \text{(A15)}$$

Using definition (A2) leads to terms analogous to (A5) and an equation analogous to (A6), except that the coefficients in (A6) are now defined by

$$a_p = S\Bigg[1 - \sum_{n=1}^{N-1}\sum_{n'=n+1}^{N}\tan\theta_n\tan\theta_{n'}\cos(\alpha_n - \alpha_{n'}) + \mathcal{O}(\tan^4\theta)\Bigg]$$

$$a_{p_\perp} = S\Bigg[\sum_{n=1}^{N-1}\sum_{n'=n+1}^{N}\tan\theta_n\tan\theta_{n'}\sin(\alpha_n - \alpha_{n'}) + \mathcal{O}(\tan^4\theta)\Bigg] \quad \text{(A16)}$$

$$C_c = S\Bigg[\sum_{n=1}^{N}\tan\theta_n\cos\alpha_n + \mathcal{O}(\tan^3\theta)\Bigg]$$

$$C_s = S\Bigg[\sum_{n=1}^{N}\tan\theta_n\sin\alpha_n + \mathcal{O}(\tan^3\theta)\Bigg].$$

Thus the formulae for α_a and θ_a still have the same form as (A12) and (A13). We note that in the low-frequency limit, only the terms proportional to $\tan\theta$ and $\tan^2\theta$ need be retained, leading to relatively compact expressions for this more complicated case.

Determination of null directions of ϕ_p

We term the null directions those values of ϕ_p for which the initial polarization is left virtually unchanged by the splitting operators. In the case of two layers this corresponds to setting the term multiplying $\hat{\mathbf{p}}_\perp$ in eq. (A6) equal to 0. Since $a_{p_\perp}$ and C_s are both real, they must both be zero. $a_{p_\perp} = 0$ is satisfied by either $\theta_1 = n\pi$ or $\theta_2 = n\pi$, or $\alpha_2 - \alpha_1 = n\pi$. But $a_{p_\perp}$ is not a function of ϕ_p so that there will be no special null directions. $C_s = 0$ gives the closest case to a null, and it can be satisfied exactly for

$$\frac{\tan\theta_2}{\tan\theta_1} = -\frac{\sin\alpha_1}{\sin\alpha_2}. \quad \text{(A17)}$$

For example, if $\theta_2 = \theta_1$, then the 'null' directions will be halfway between the two fast directions. Because $a_{p_\perp}$ is only identically zero for special kinds of anisotropy, the $\hat{\mathbf{p}}_\perp$ component will never be identically zero in general. However, we note that it is quadratic in ω, and hence at low frequency it will be small compared to the other terms. Thus (A17) should approximately give the location of the null direction.